Supporting Information

TABLE OF CONTENTS

Materials and general methods

All the reagents, chemicals, and solvents were purchased from Sigma Aldrich, Tokyo Chemical Industries (TCI), and AVRA only. The purchased chemicals were used without further purification. UV-Visible 1800 Shimadzu spectrometer and Agilent, Cary Eclipse Spectrophotometer were used to record the UV-Vis absorption and fluorescence emission spectra, respectively. UV-Vis absorption and fluorescence emission study were performed using a quartz cuvette of path length 1 cm. The photo images were taken in visible light as well as under UV light at 365 nm. The density functional theory (DFT) and time-dependent density functional theory (TD-DFT) studies are performed using the Gaussian 16 *ab initio*/DFT quantum chemical simulation package and the B3LYP/6-31G* level of theory. The Stern-Volmer plot for the calculation of the quenching constant (K_{SV}), the Benesi-Hildebrand plot, the calibration plot for the calculation of limit of detection (LOD), and Job's plot of compound **1** were plotted by using the fluorescence titration experiment with the gradual addition of TFA from 0 to 4 equivalents at an excitation wavelength of 370 nm in $CHCl_3$ solution.

Synthesis

The molecules **TPE, 4-NO_2 TPE,** and **4-NH_2 TPE** were synthesized from the reported literature method.[1] Firstly, nitration of **TPE** was undertaken by using concentrated nitric acid in acetic acid at reflux for 12 h to form the compound **4-NO_2 TPE**. The formed compound, **4-NO_2 TPE,** was reduced to **4-NH_2 TPE** by using hydrazine hydrate and Pd/C in ethanol at 80 °C for overnight under an N_2 atmosphere (Scheme S1).

Synthesis of 4,4',4'',4'''-(ethene-1,1,2,2-tetrayl)tetrakis(N,N-dimethylaniline) (1)

To a benzene and water (7:1) solution (20 mL), 4,4',4'',4'''-(ethene-1,1,2,2-tetrayl)tetraaniline (**4-NH_2 TPE**) (0.2 g, 0.5 mmol), tetra-n-butylammonium iodide (0.104 g, 0.28 mmol), potassium hydroxide (0.286 g, 5 mmol), was added and stirred for 5 min. Iodomethane (0.32 mL, 5 mmol) was added dropwise at room temperature with constant stirring. Further, the reaction mixture was

heated at 90 °C till the completion of the reaction. The organic layer was extracted with $CHCl_3$, washed several times with water and saturated sodium carbonate solution, and dried over sodium sulfate. The organic layer was concentrated under a vacuum and purified through column chromatography using ethyl acetate: pet-ether (20:80, v/v ratio) as an eluent to get a final compound **1** as a light green-coloured solid.

Yield (0.12 g, 47%). Light green-coloured solid. M. P. 152-155 °C. ^{1}H NMR (DMSO-d_6, 400 MHz) δ ppm: 7.61 (d, 2H, J = 8.8 Hz), 6.77 (d, 2H, J = 8.8 Hz), 3.02 (s, 6H). ^{13}C NMR (DMSO-d_6, 400 MHz) δ ppm: 192.6, 153.0, 131.9, 125.7, 111.1, 40.1.

Synthetic scheme

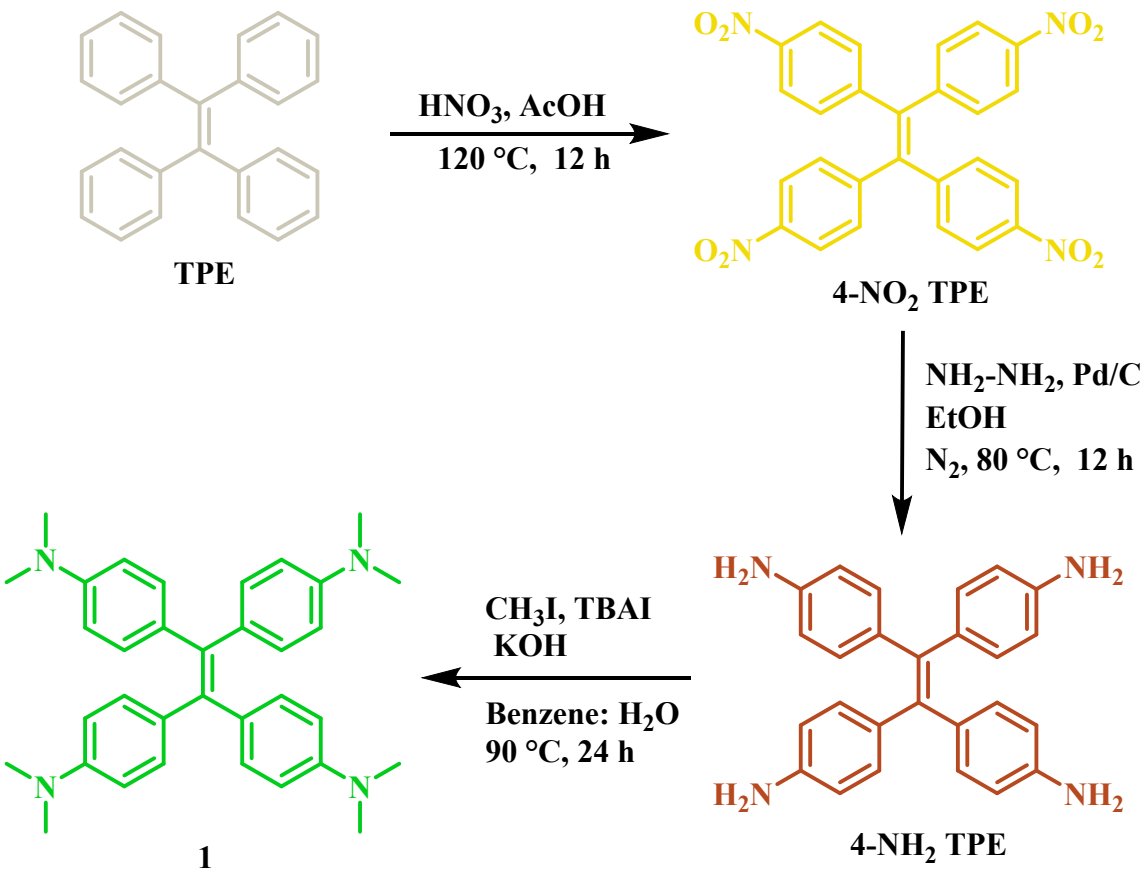

Scheme S1. Synthetic scheme of compound **1**.

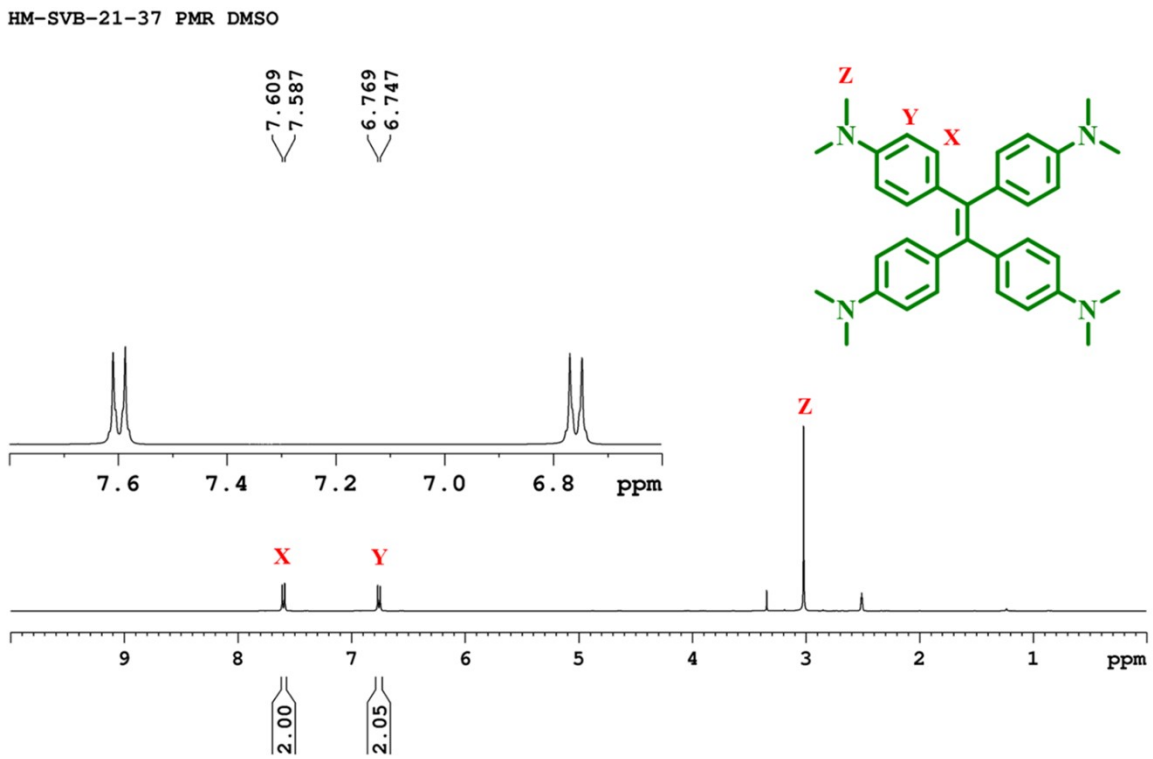

Figure S1a. ^{1}H NMR of compound **1**

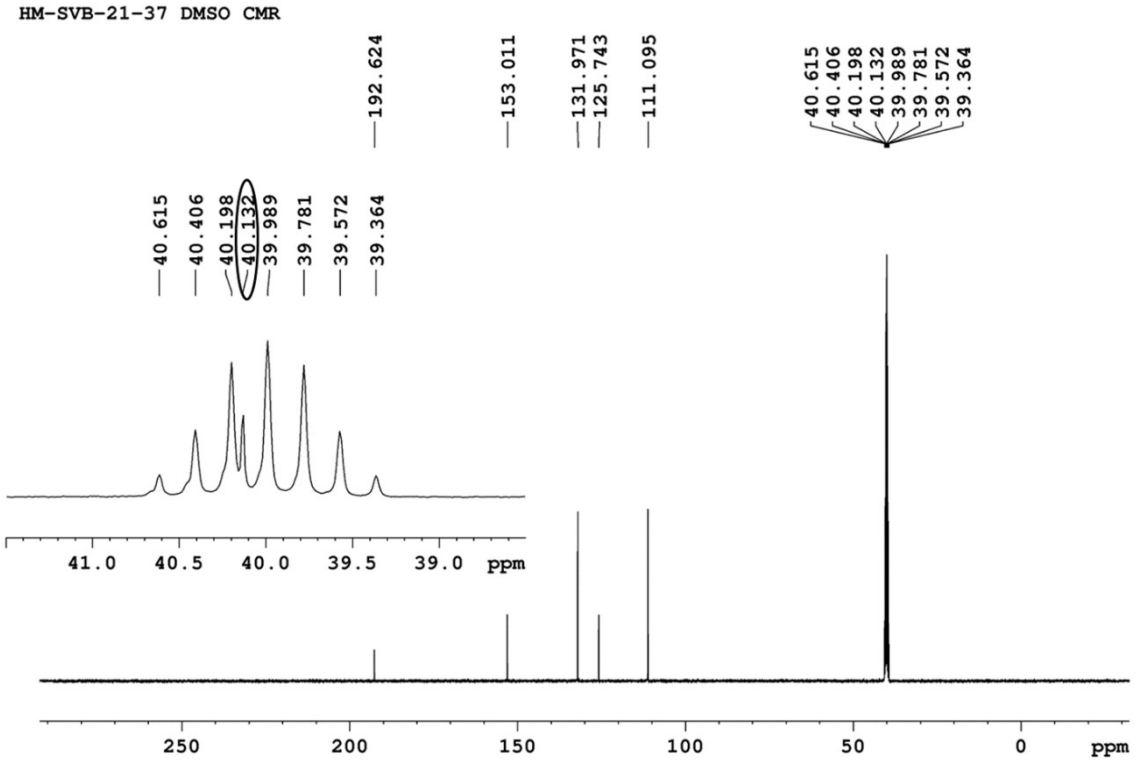

Figure S1b. ^{13}C NMR of compound **1.**

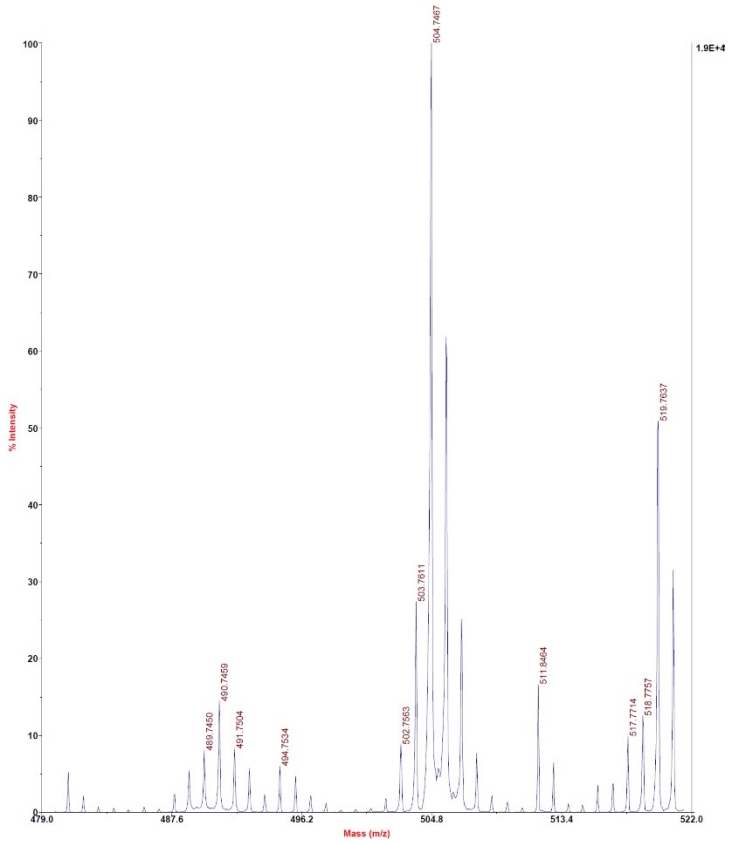

Figure S2. Mass of compound **1.**

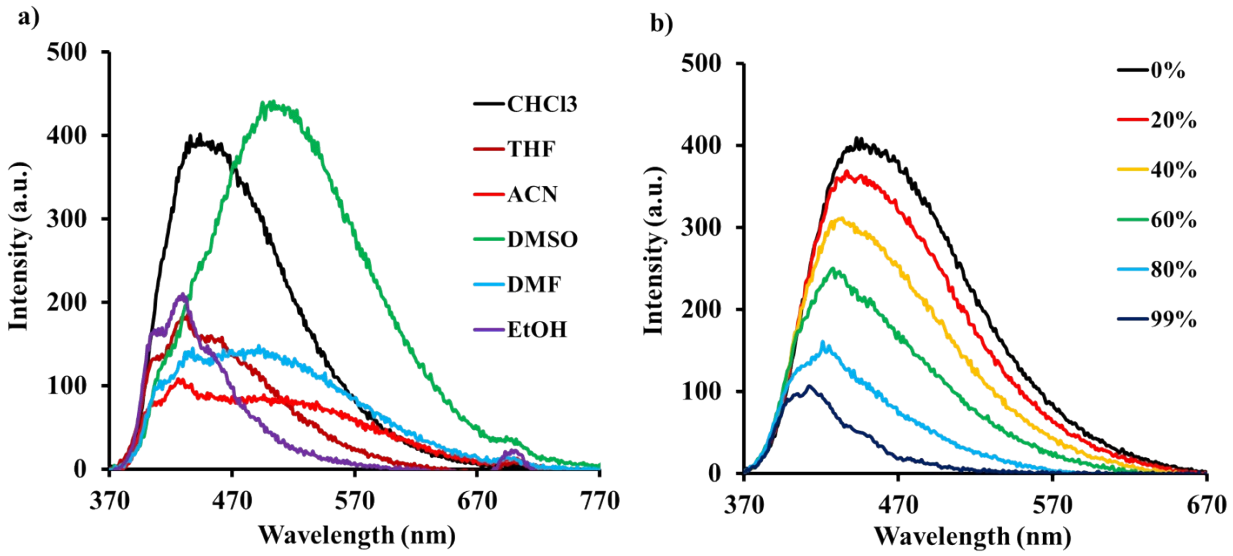

Figure S3. (a) Fluorescence emission response of **1** in different solvents. (b) The study of aggregation-induced emission (AIE) activity of **1** by recording the fluorescence emission (2×10^{-5} M) in $CHCl_3$:Hexane mixture.

Mechanochromic studies

The mechanochromic properties of **1** were studied by employing the physical processes: grinding, fuming, and heating, with a change in colour of the fluorescence emission recorded under UV light at 365 nm, and the results were illustrated in Figure S4. As shown in Figure S4, probe **1** exhibits light green fluorescence in its solid form. However, upon grinding, the colour of the fluorescence emission of **1** is changed from green to light blue due to the change in the crystalline size of **1**. Furthermore, half a portion of grinded compound **1** fumed with acetone, reverting to its original light-yellow colour intensity. Later, the remaining portion of grinded compound **1** was heated, and after heating, the fluorescence emission colour changed from light blue to dark blue under UV light at 365 nm excitation.

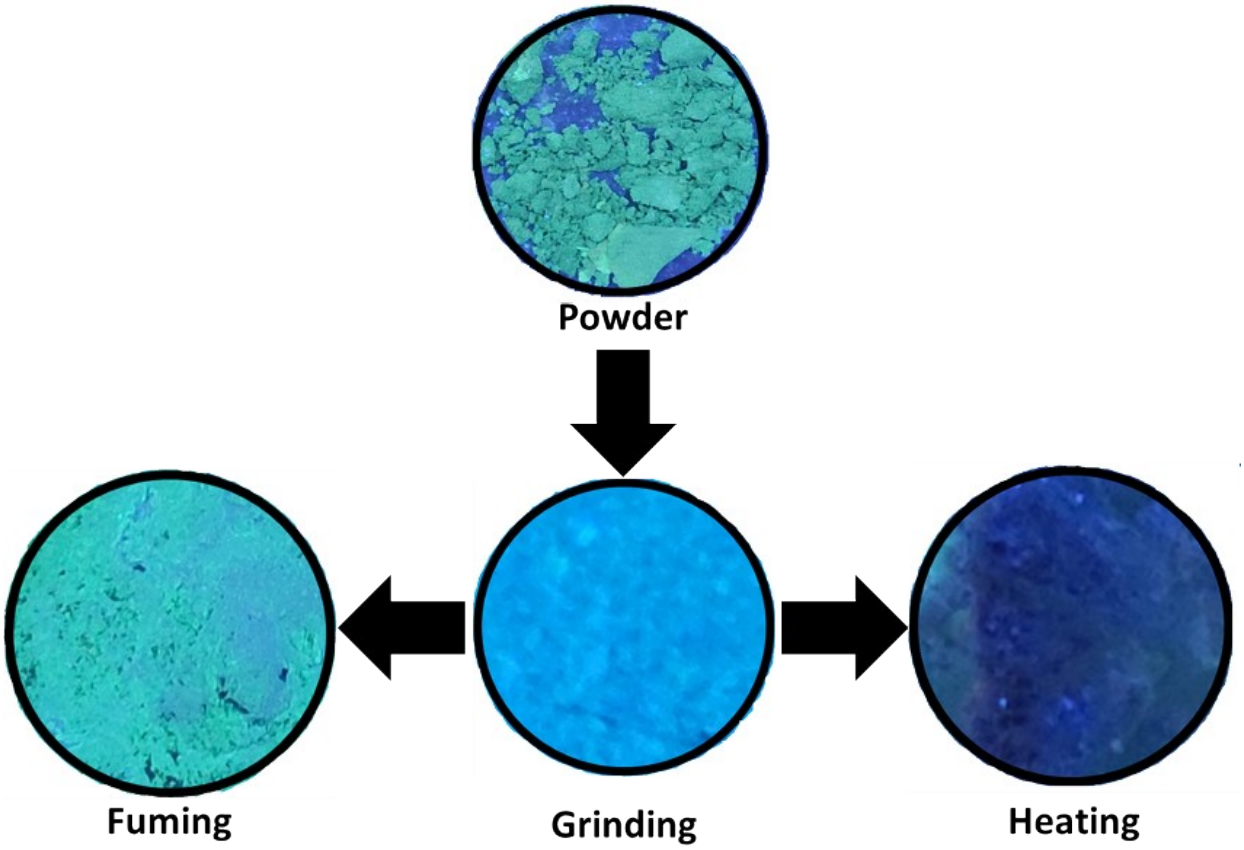

Figure S4. Study of mechanochromic properties of compound **1** displaying the changes in its fluorescence emission on grinding, fuming, and heating.

Density Functional Theory (DFT) studies

The results of the computational calculations are obtained using the Gaussian 16 *ab initio*/DFT quantum chemical simulation package.[2] The geometry optimization of the molecules compound **1** and compound **1** + 4H is carried out at the B3LYP/6-31G* level. The frontier molecular orbitals (FMO) are generated using Avogadro[3,4] and are given in Figures 3a, b and S5. The optimized geometries are considered for the time-dependent density functional theory (TD-DFT) studies using the B3LYP/6-31G* level of theory. TD-DFT results were analyzed by employing the Gauss-Sum program,[5] TD-DFT results obtained are reported in Table S1. From the TD-DFT results, it is seen that the absorption of compound **1** is at 410, 380 nm, and compound **1** + 4H is at 332, 285 nm, as shown in Figure S6. The frequency calculations also have been performed to confirm the minima. The polarizable continuum model (PCM) is used to investigate the effect of solvent ($CHCl_3$) for charge transfer excitation study.

Compound **1**			
Sr. No	**Orbital number**	**Energy (eV)**	**Orbital Picture**
1	141(L+4)	0.546eV	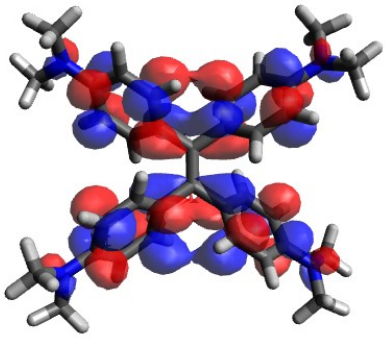
2	139(L+2)	0.201eV	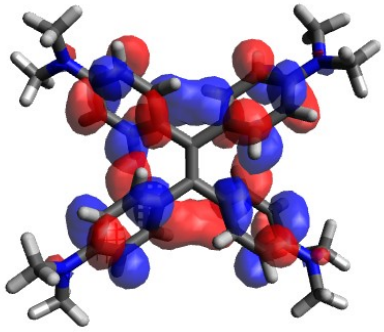

3	137(L)	-0.734eV	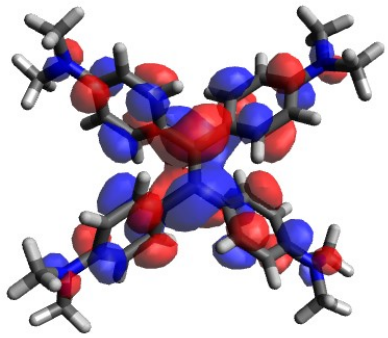
4	136(H)	-4.227eV	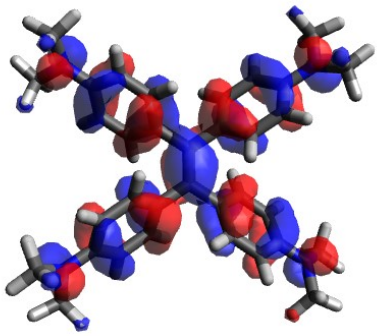
5	134(H-2)	-5.112eV	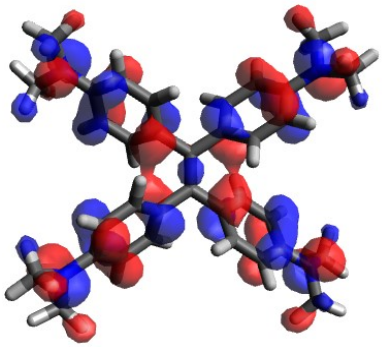

Figure S5a. Frontier molecular orbitals of compound **1** with energy in eV.

Compound **1** + 4H

Sr. No	**Orbital number**	**Energy (eV)**	**Orbital Picture**

1	138(L+1)	-3.155eV	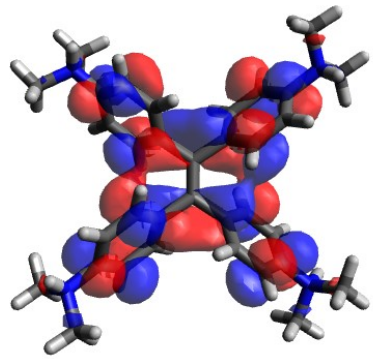
2	137(L)	-3.903eV	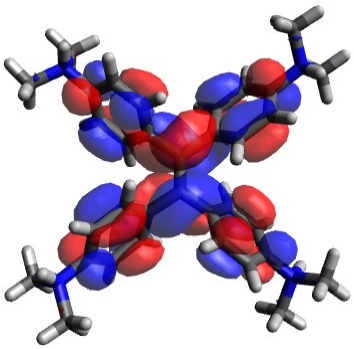
3	136(H)	-8.159eV	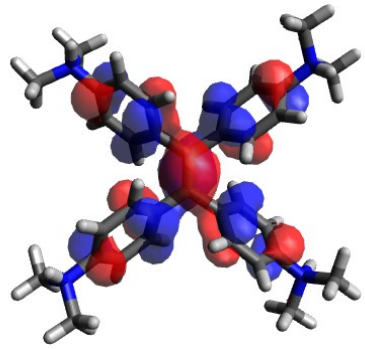

Figure S5b. Frontier molecular orbitals of compound **1** + 4H with energy in eV.

Figure S5. Frontier molecular orbitals of compound **1** and compound **1** + 4H.

Table S1. Calculated TD-DFT excitations for the most stable conformations of compound **1** and compound **1** + 4H.

Molecules	Excitation Wavelength (nm)	Oscillator Strength (f)	Excitations	Percentage Contribution for transition

Compound **1**	410	0.6343	136 ->137	HOMO->LUMO (100%)
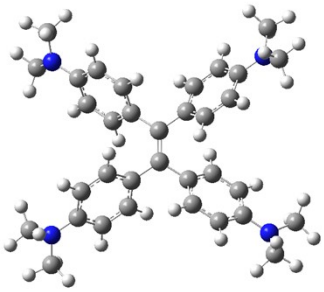	318	0.5743	134 ->137	H-2->LUMO (30%),
			136 ->139	HOMO->L+2 (65%)
			136 ->141	HOMO->L+4 (3%)
Compound **1** + 4H				
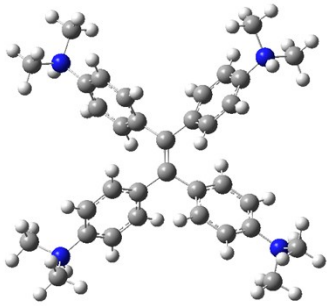	332	0.6193	136 ->137	HOMO->LUMO (99%)
	285	0.2835	136 ->138	HOMO->L+1 (95%)

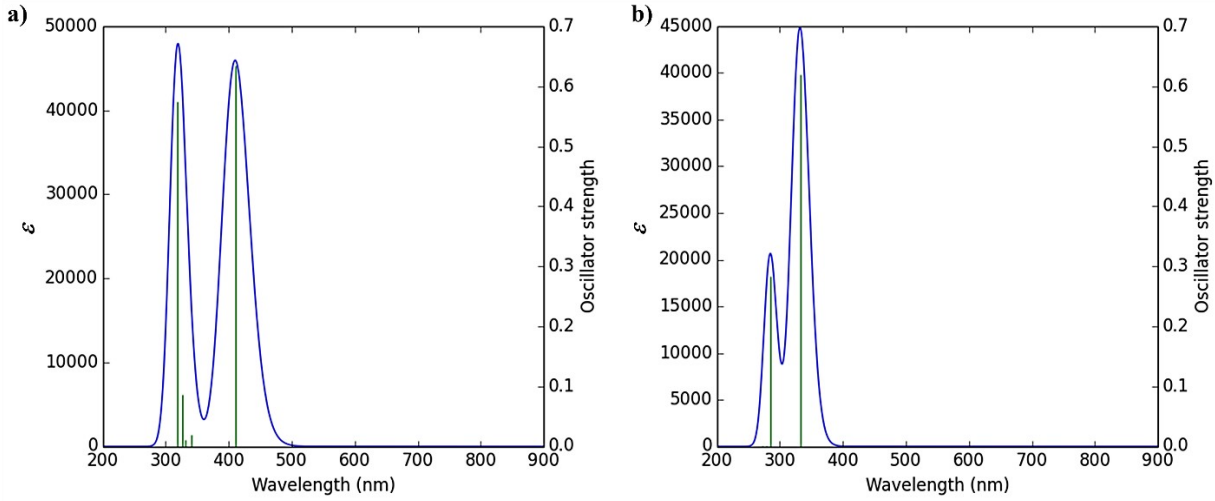

Figure S6. The computed absorption spectrum of (a) compound **1** and (b) compound **1** + 4H.

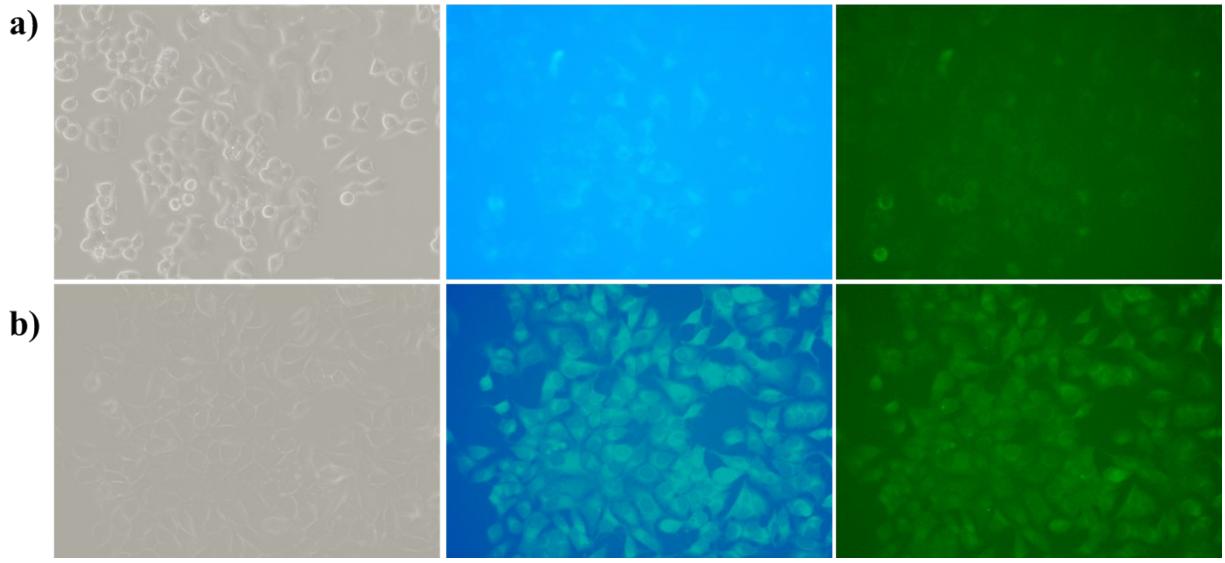

Figure S7. The MCF7 cells (a) without compound **1** and (b) with compound **1** at neutral pH.

Table S2: Comparison of LOD, reversibility, test strip, and biological study of **1** with previously reported molecules.

Sr. No	**Compound**	**Sensing method**	**LOD**	**Test strip / TLC plate**	**Reversibility**	**Bio. Study**	**Ref.**
1	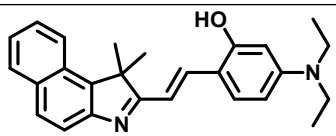	Fluorescence Turn ON	2.96 μM	No	No	Yes	6
2	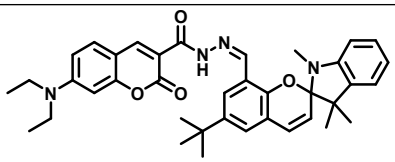	Colourimetric and fluorescence	-	No	Yes	Yes	7
3	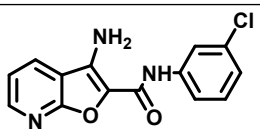	Fluorescence	-	No	No	No	8
4	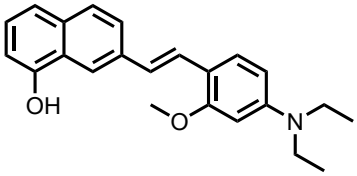	Fluorescence	-	No	No		9

5	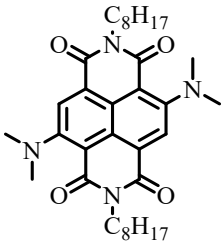	Fluorescence Turn ON	2.77 nM	Yes	Yes	No	10
6	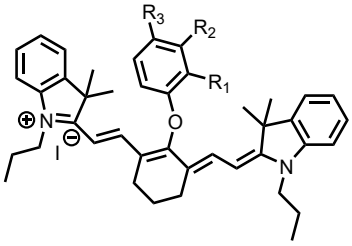	Fluorescence	-	No	Yes	Yes	11
7	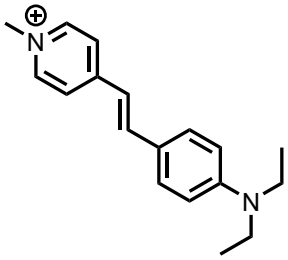	Fluorescence Turn OFF	-	No	Yes	Yes	12
8	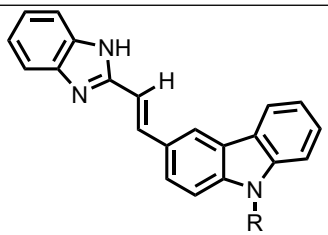	Fluorescence	-	No	Yes	Yes	13
9	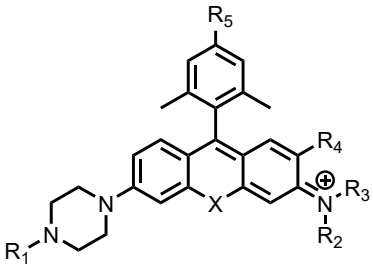	Fluorescence	-	No	No	Yes	14
10	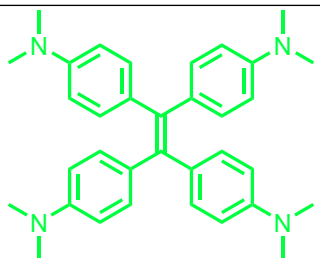	**Fluorescence Turn OFF**	**6.9 µM**	**Yes**	**Yes**	**Yes**	**This work**

References

1 S. Medina Rivero, P. García Arroyo, L. Li, S. Gunasekaran, T. Stuyver, M. J. Mancheño, M. Alonso, L. Venkataraman, J. L. Segura and J. Casado, *Chemical Communications*, 2021, **57**, 591–594.

2 M. J. Frisch, G. W. Trucks, H. B. Schlegel, G. E. Scuseria, M. A. Robb, J. R. Cheeseman, G. Scalmani, V. Barone, G. A. Petersson and H. Nakatsuji, *Inc., Wallingford CT*.

3 Avogadro: an open-source molecular builder and visualization tool. Version 1.1.0. http://avogadro.openmolecules.net/

4 M. D. Hanwell, D. E. Curtis, D. C. Lonie, T. Vandermeersch, E. Zurek and G. R. Hutchison, *SOFTWARE Open Access Avogadro: an advanced semantic chemical editor, visualization, and analysis platform*, 2012, vol. 4.

5 N. M. O'Boyle, A. L. Tenderholt and K. M. Langner, *J Comput Chem*, 2008, **29**, 839–845.

6 Y. Zhang, Y. Zhao, A. Zhou, Q. Qu, X. Zhang, B. Song, K. Liu, R. Xiong and C. Huang, *Spectrochim Acta A Mol Biomol Spectrosc*, DOI:10.1016/j.saa.2021.120014.

7 X. He, W. Xu, C. Xu, F. Ding, H. Chen and J. Shen, *Dyes and Pigments*, DOI:10.1016/j.dyepig.2020.108497.

8 L. Zhang, Y. Liu, X. Li, Y. Guo, Z. Jiang, T. Jiao and J. Yang, *ACS Omega*, 2021, **6**, 4800–4806.

9 S. Guria, A. Ghosh, T. Mishra, M. Kumar Das, A. Adhikary and S. Adhikari, *J Photochem Photobiol A Chem*, DOI:10.1016/j.jphotochem.2020.113074.

10 V. G. More, D. N. Nadimetla, G. A. Zalmi, V. K. Gawade, R. W. Jadhav, Y. D. Mane and S. v. Bhosale, *ChemistryOpen*, DOI:10.1002/open.202200060.

11 H. Mai, Y. Wang, S. Li, R. Jia, S. Li, Q. Peng, Y. Xie, X. Hu and S. Wu, *Chemical Communications*, 2019, **55**, 7374–7377.

12 N. Wang, X. Yu, T. Deng, K. Zhang, R. Yang and J. Li, *Anal Chem*, 2020, **92**, 583–587.

13 J. Ge, L. Fan, K. Zhang, T. Ou, Y. Li, C. Zhang, C. Dong, S. Shuang and M. S. Wong, *Sens Actuators B Chem*, 2018, **262**, 913–921.

14 S. Takahashi, Y. Kagami, K. Hanaoka, T. Terai, T. Komatsu, T. Ueno, M. Uchiyama, I. Koyama-Honda, N. Mizushima, T. Taguchi, H. Arai, T. Nagano and Y. Urano, *J Am Chem Soc*, 2018, **140**, 5925–5933.